ARID4B loss leads to activated STAT1-dependent interferon pathway in mouse embryonic stem cells and during meso/endodermal differentiation

Nihal Terzi Çizmecioğlu

Department of Biological Sciences, Middle East Technical University, Faculty of Arts and Sciences, Ankara, Turkey

Abstract

Objective: Proper deactivation of the pluripotency network and activation of a lineage-specific gene expression program are critical for mouse embryonic stem cell (mESC) differentiation. This is achieved by the coordinated action of transcription and chromatin factors. Our previous work identified ARID4B as a critical chromatin factor for mesoderm and endoderm differentiation. As part of a histone deacetylase complex, ARID4B plays a role in transcriptional suppression of its direct targets. Here, we investigated the mechanism of ARID4B function in mESC differentiation by focusing on genes and pathways that are upregulated in its absence.

Material and Methods: We analyzed transcriptomic results of wild-type and arid4bΔ endoderm or mesoderm differentiated cells through integrative genomics viewer and ingenuity pathway analysis. We performed real-time quantitative polymerase chain reaction for selected genes. To understand pathway activation, we performed Western blot for candidate proteins during the time-course of differentiation. We also analyzed H3K4me3, H3K27me3 and H3K27Ac ChIP-seq results to understand changes in the chromatin environment.

Results: Interferon-related genes were activated in arid4bΔ mESCs and endoderm or mesoderm directed cells. Consistent with this, higher phosphorylated STAT1 levels were found in arid4bΔ mESCs while a related phosphorylated STAT3 was unchanged. Finally, we observed a significant increase in H3K4me3 around interferon-related distal gene regulatory regions with a combination of either upregulation of H3K27Ac level or downregulation of H3K27me3 level.

Conclusion: These results provide evidence that ARID4B is involved in the suppression of interferon-related genes in mESCs and during meso/endoderm differentiation through modulation, mainly of H3K4me3. This regulation might be important for successful mESC differentiation.

(J Turk Ger Gynecol Assoc 2023; 24: 187-96)

Keywords: Embryonic stem cell, differentiation, chromatin, interferon, STAT1

Received: 11 July, 2023 **Accepted:** 26 July, 2023

Introduction

Embryonic stem cells (ESC) originate from the blastocyst stage of the developing embryo. They possess self-renewal ability and pluripotency, which make them invaluable in vitro models for studies focusing on early embryonic development. While self-renewal enables culturing ESCs almost indefinitely, through their pluripotent nature, ESCs can be directed to differentiate towards any lineage in vitro. Mimicking embryonic development, ESC commitment towards mesoderm, endoderm and neuroectoderm can be achieved with the carefully timed use of a combination of cytokines (1,2).

ESC stage is established and maintained by pluripotency transcription factors (TF), such as OCT4, SOX2, NANOG and KLF4 (3). During ESC differentiation, the pluripotency network achieved by these TFs need to be shut off while a lineage-specific gene expression program is established. Activation of lineage-specific genes poses a challenge, since their chromatin environment is not permissive of transcription at the ESC stage. Therefore, TFs that initiate differentiation need to gain

Address for Correspondence: *Nihal Terzi Çizmecioğlu*
e.mail: nterzi@metu.edu.tr ORCID: orcid.org/0000-0001-5778-764X

DOI: 10.4274/jtgga.galenos.2023.2023-7-5

access to their gene regulatory sequences at the promoter and enhancers and increase the accessibility of these regions to downstream transcription related machinery. The lineage-specific TFs that start this cascade of events are called pioneer TFs (4). Endoderm lineage originates from a mesodermal embryonic structure called the primitive streak and thus share an early common differentiation path (5,6). Neuroectoderm, on the other hand, is distinct from meso/endodermal lineages (7). BRACHYURY (Bry) was identified as a pioneer TF for mesodermal lineage and is used as a marker gene for meso/endodermal commitment. Similarly, FOXA2 is a pioneer TF for definitive endodermal lineage.

TFs instigate ESC differentiation by alteration of the target gene chromatin environment (8). Eukaryotic chromatin is made up of repeating units of conserved proteins called histones (9). Two copies of histones 2A, 2B, 3 and 4 form nucleosomes that wrap the genomic DNA. Modifications of histones at particular modifiable amino-acids, the number or the positioning of nucleosomes across the gene region, the use of histone variants in the nucleosome structure or methylation of DNA can change the chromatin environment and alter the frequency or efficiency of transcription.

Histones can be methylated at lysine or arginines, acetylated at lysines and phosphorylated at serine or threonines (9). Modification itself, as well as the exact residue that gets modified, can have profound effects on transcription. For example, histone acetylation leads to weakening of interaction between nucleosomes and DNA. High levels of histone acetylation, especially around promoter regions, help create an accessible environment for recruitment of factors critical for transcription initiation. Thus, histone acetylation generally correlates with active transcription, although acetylation in specific lysines can have unique outcomes. The effect of histone methylation depends on the level of methylation (mono, di or trimethylation) and which residue is methylated. While H3K4me3 is generally observed over transcriptionally active gene regions, H3K27me3 plays a suppressive role.

During differentiation, lineage-specific genes become more accessible and start harboring histone modifications that correlate with active transcription such as high level of histone acetylation including H3K27Ac and H3K4me3. Pluripotency genes are instead suppressed with repressive histone modifications, such as H3K27me3 or DNA methylation (10).

Our previous study focused on chromatin factors that regulate mouse embryonic stem cells (mESC) differentiation (11). We identified ARID4B as an important factor that is required for both mesoderm and endoderm commitment. In its absence, mESCs fail to express critical pioneer TFs for these lineages and cannot instigate differentiation. The failure of meso/endodermal differentiation was not due to improper pluripotency network shut-off. Instead, ARID4B loss resulted in accumulation of repressive H3K27me3 histone markers on lineage-specific genes.

As part of an RPD3 histone deacetylase complex, ARID4B regulates the overall histone acetylation landscape, primarily around promoter and enhancer regions (12). Histone acetylation levels around regulatory regions can impact transcriptional output by altering their accessibility to binding of other critical factors. ARID4B lacks any enzymatic domain but has a DNA and various protein-protein interaction domains. Particularly, the presence of TUDOR, PWWP and chromobarrel domains indicate interactions with modified histones and chromatin in general. DNA binding is mediated through its AT-rich interaction domain (ARID) in a sequence-independent manner. Recruitment of ARID4B along with the rest of the RPD3 complex generally leads to transcriptional suppression of target genes through histone deacetylation. In order to further delineate the mechanism of ARID4B function in mESC differentiation, we therefore decided to focus on pathways that are activated in the absence of ARID4B.

Material and Methods

mESC culture and differentiation

The study was done using already established mESC lines. Therefore, ethics committee approval form or institutional review board forms were not required. ARID4B knockout mESCs were prepared previously (11). Wild-type and arid4bΔ mESCs were cultured using standard serum containing medium on irradiated MEFs (13). mESC differentiation towards mesoderm and endoderm was performed using previously optimized protocols (11,14).

Transcriptomic analysis and RT-qPCR

RNA extraction, cDNA synthesis and quantitative polymerase chain reaction (qPCR) were done using previously published protocols (11). rRNA minus RNA-sequencing was previously performed (11). The transcriptomic data is available at NCBI GEO (GSE153633). Primers used for real-time quantitative polymerase chain reaction (RT-qPCR) are listed in Table 1.

Western blot

Cellular extract preparation and Western blot was done using previously published protocols (11). Antibodies used were: ARID4B (Bethyl Laboratories, A302-233A), ACTIN (Millipore, MAB1501), STAT1 (CST, 9172), pSTAT1 (CST, 9167), STAT3 (CST, 9139), pSTAT3 (CST, 9145).

Chromatin immunoprecipitation-sequencing and analysis

H3K4me3, H3K27Ac and H3K27me3 chromatin immunoprecipitation (ChIP)-seq experiments and subsequent

data analysis were previously performed in wild-type and arid4bΔ cells on day 5 of endoderm differentiation (11,15). Sequencing data is available at NCBI GEO (GSE153634).

Statistical analysis

Experiments were conducted with three independent biological replicates. RNA-seq and ChIP-seq experiments, the statistical analysis was done within the analysis package (11). Algorithms used within the study, such as Ingenuity Pathway Analysis (IPA), Gene Set Enrichment Analysis (GSEA) and Genomic Regions Enrichment of Annotations Tool (GREAT) have their own statistical analysis embedded within and were used as default. RT-qPCR results were graphed using GraphPad Prism Software and statistically analyzed using Student's t-test (*: $p \leq 0.05$, **: $p \leq 0.01$, ***: $p \leq 0.001$).

Results

Meso/endodermal differentiation defect observed in arid4bΔ mESCs might stem either from pathways that cannot be turned on or from those that are aberrantly upregulated. Our previous studies had focused on which pathways and functions were lost in arid4bΔ mESCs as they differentiate towards meso/endoderm lineages. In this paper, we decided to investigate abnormally upregulated functions.

We had previously optimized the embryoid body-based mesoderm and endoderm differentiation protocol and could observe upregulation of pioneer TFs for either lineage by day 5 of differentiation (14). arid4bΔ mESCs could not induce the expression of these TFs, leading to meso/endodermal commitment defect (11). RNA-seq analysis of day 5 samples from wild-type or arid4bΔ cells showed no apparent increase in meso/endoderm related signaling and gene expression pathways. Inappropriate pathway induction in arid4bΔ cells might hinder successful differentiation. We, therefore, looked for pathways that are enriched in the differentially upregulated genes in arid4bΔ cells over wild-type cells on day 5 of endoderm differentiation. IPA (Qiagen) revealed interferon signaling, activation of cytosolic pattern recognition receptors and the role of pattern recognition receptors in recognition of bacteria and viruses as the most enriched pathways (Figure 1a). Similarly, GSEA (the Broad Institute) showed cellular defense response and interferon α/β signaling as aberrantly upregulated in arid4bΔ cells (Figure 1b, c). Additionally, the IRF TF motif was found to be enriched in genes that were more expressed in arid4bΔ cells over wild-type (Figure 1d). The overrepresentation of innate immune response-specific genes (red dots) in arid4bΔ cells was visualized using the volcano-plot (Figure 1e, Table 2) and Integrative Genomics Viewer [(IGV), the Broad Institute] (Figure 1f-k).

We wondered whether ARID4B loss would lead to a similar upregulation of interferon signaling in mesoderm differentiation. To investigate this hypothesis, we directed wild-type and arid4bΔ mESCs towards mesodermal lineage and assessed differentiation success using the induction of mesodermal pioneer TF BRACHYURY. arid4bΔ mESCs were unable to express BRACHYURY, as well as its downstream target genes (11). IPA and GSEA similarly identified interferon signaling and activation of IRF by cytosolic pattern recognition receptors among top canonical pathways in arid4bΔ cells (Figure 2a-c). However, volcano plot representation showed that the interferon signaling related genes were not as highly expressed in mesoderm as they were in endoderm (Figure 2d, Table 3). Regardless, they showed apparent upregulation in arid4bΔ cells compared to wild-type (Figure 2e-j). These results collectively point to a role of ARID4B in suppression of interferon response during ESC differentiation towards meso/endodermal lineages.

The next step was to validate transcriptomic data and perform RT-qPCR for a list of highest differentially upregulated genes in arid4bΔ cells. Interferon induced transmembrane protein encoding *IFITM3* was the top of this list and showed clear induction upon ARID4B loss on day 5 of endoderm differentiation (Figure 3a). As the major interferon signaling mediator, *STAT1* was expressed markedly higher in arid4bΔ endodermal cells (Figure 3b). Cytosolic dsRNA sensor *DDX58* (RIG-I) and related antiviral protein encoding *DDX4* were similarly upregulated (Figure 3c, d). The expression of these genes was still significantly higher than wild-type in mesoderm commitment (Figure 3e-h) but their fold induction was more severe during endoderm differentiation. Therefore, we focused on endoderm differentiation hereafter.

To this point, results had been obtained at a specific time point (day 5) during mESC differentiation. In order to gain a

Table 1. Primers used in the study

Gene	Forward primer	Reverse primer
IFITM3	CCCCCAAACTACGAAAGAATCA	ACCATCTTCCGATCCCTAGAC
STAT1	GCTGCCTATGATGTCTCGTTT	TGCTTTTCCGTATGTTGTGCT
DDX58	ATTCAGGAAGAGCCAGAGTGTC	GTCTTCAATGATGTGCTGCAC
DDX4	GGTCCAAAAGTGACATATATACCC	TTGGTTGATCAGTTCTCGAGT
B-ACTIN	ATGAAGATCCTGACCGAGCG	TACTTGCGCTCAGGAGGAGC

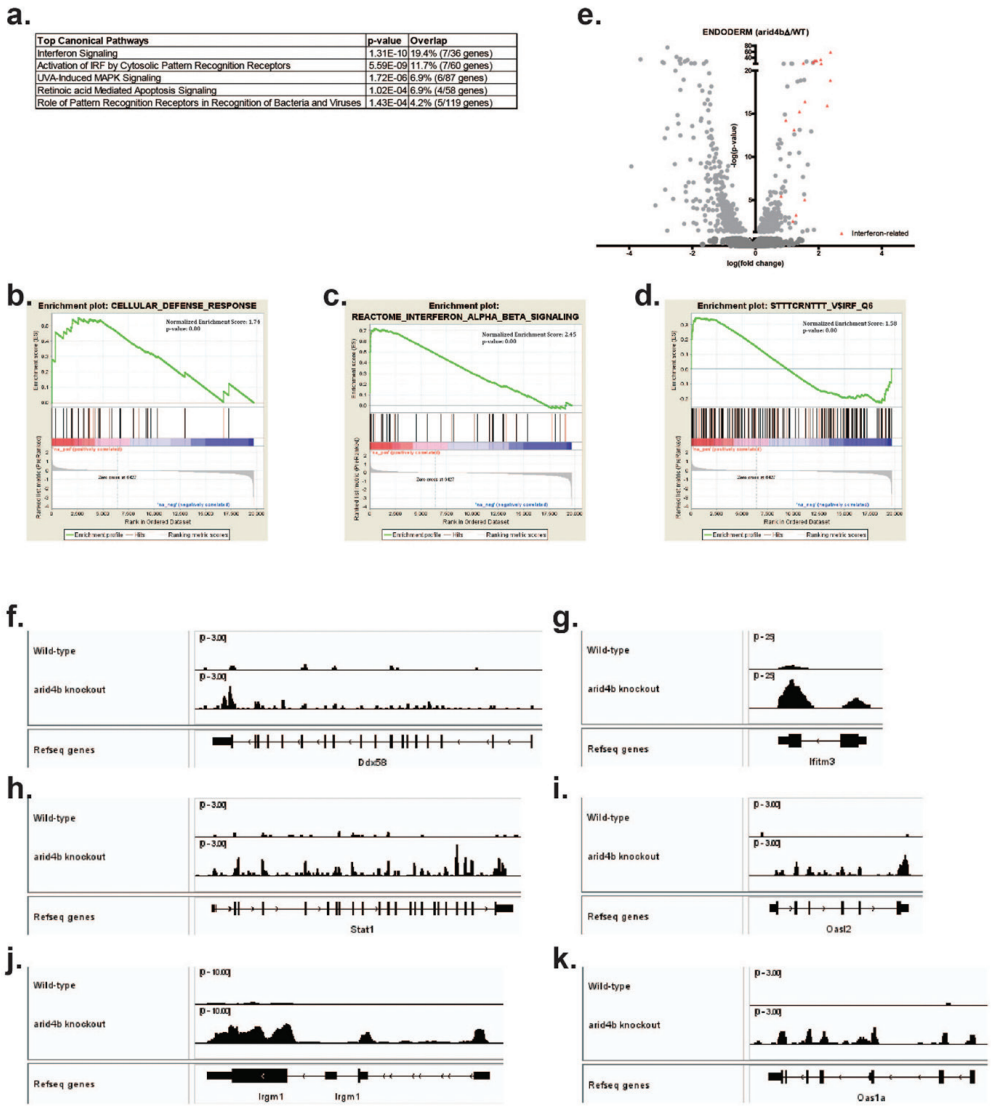

Figure 1. ARID4B loss leads to elevated expression of interferon-related genes during endoderm differentiation. Ingenuity Pathway Analysis (a) and Gene Set Enrichment Analysis (b-d) of differentially upregulated genes in arid4bΔ cells on day 5 of endoderm differentiation, (e) Volcano plot representation of RNA-seq data (day 5 of endoderm differentiation, arid4bΔ/wild-type). Red triangles show interferon-related genes., Integrative Genomics Viewer visualization of *DDX58* (f), *IFITM3* (g), *STAT1* (h), *OASL2* (i), *IRGM1* (j) and *OAS1A* (k) using RNA-seq data

more detailed understanding of aberrant induction kinetics of immune-related genes in arid4bΔ cells, RT-qPCR analysis was performed in wild-type and arid4bΔ mESCs through the time course of endoderm differentiation. At the mESC stage (depicted as day 0 of differentiation in graphs), *IFITM3* was already highly expressed in arid4bΔ cells, although the fold difference seemed to increase later during endoderm differentiation (after day 3) (Figure 3i). *STAT1* showed a highly variable but elevated expression in arid4bΔ mESCs and its expression remained elevated throughout our time-course (Figure 3j). *DDX58* (RIG-I) followed a similar pattern to *STAT1* (Figure 3k) while *DDX4* levels were similar between wild-type and arid4bΔ mESCs and became elevated in arid4bΔ cells only late in endoderm differentiation (Figure 3l). These results show that ARID4B loss leads to higher interferon-related gene expression at the mESC stage and this effect gets stronger through the endoderm differentiation time-course with variable kinetics and extent for each target gene.

Transcriptional upregulation might not necessarily lead to protein level alterations and pathway activation. To understand whether observed increased transcripts activate interferon signaling in arid4bΔ cells, we performed Western blot using total cell lysates of mESCs (day 0 of differentiation) and during the time course of endodermal differentiation. Cytosolic

Table 2. RNAseq results of interferon-related genes in endoderm differentiated cells

Rank in arid4bΔ/WT	EntrezID	Gene symbol	P-adjusted	Log fold change
1	66141	*IFITM3*	3.62612E-59	2.38
2	15944	*IRGM1*	1.35974E-19	2.37
3	20846	*STAT1*	1.17823E-16	2.27
4	24110	*USP18*	9.24286E-21	2.08
5	230073	*DDX58*	1.26967E-34	2.07
6	23962	*OASL2*	6.27663E-31	1.93
7	54396	*IRGM2*	3.01479E-31	1.88
9	246730	*OAS1A*	1.32575E-25	1.83
16	17858	*MX2*	4.03169E-17	1.57
17	15957	*IFIT1*	9.14703E-06	1.56
20	19106	*EIF2AK2*	2.58357E-22	1.52
26	23960	*OAS1G*	5.80493E-16	1.39
33	15959	*IFIT3*	0.000560908	1.29
36	234311	*DDX60*	7.47842E-14	1.22
38	19039	*LGALS3BP*	0.002821116	1.18
51	56417	*ADAR*	5.944E-15	0.96
68	16391	*IRF9*	3.55256E-06	0.81

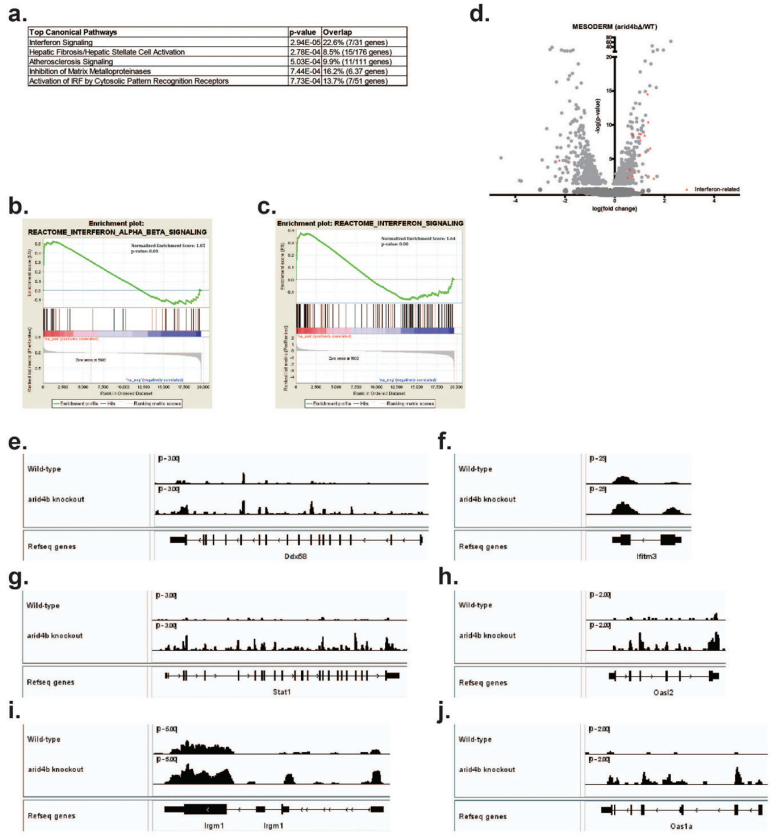

Figure 2. ARID4B loss leads to elevated expression of interferon-related genes during mesoderm differentiation. Ingenuity Pathway Analysis (a) and Gene Set Enrichment Analysis (b, c) of differentially upregulated genes in arid4bΔ cells on day 5 of mesoderm differentiation, (d) Volcano plot representation of RNA-seq data (day 5 of mesoderm differentiation, arid4bΔ/wild-type). Red triangles show interferon-related genes., Integrative Genomics Viewer visualization of *DDX58* (e), *IFITM3* (f), *STAT1* (g), *OASL2* (h), *IRGM1* (i) and *OAS1A* (j) using RNA-seq data

Table 3. RNAseq results of interferon-related genes in mesoderm differentiated cells

Rank in ARID4BΔ/WT	EntrezID	Gene symbol	P-adjusted	Log fold change
4	15959	*IFIT3*	0.007579062	1.57
7	20846	*STAT1*	2.6319E-07	1.43
10	24110	*USP18*	3.82944E-11	1.35
13	246730	*OAS1A*	2.92352E-15	1.32
14	15957	*IFIT1*	0.002376266	1.25
19	23962	*OASL2*	3.40716E-09	1.20
30	230073	*DDX58*	2.11369E-09	1.05
32	54396	*IRGM2*	1.7808E-08	1.02
33	234311	*DDX60*	2.49212E-06	1.02
43	23960	*OAS1G*	1.81248E-09	0.98
63	15958	*IFIT2*	0.001007765	0.81
80	56417	*ADAR*	2.45002E-09	0.75
88	100038882	*ISG15*	0.003604275	0.72
90	66141	*IFITM3*	3.13061E-09	0.72
143	16391	*IRF9*	0.000478808	0.62
154	19106	*EIF2AK2*	0.00028144	0.60
211	23961	*OAS1B*	0.005215998	0.52

double-stranded viral RNAs are recognized by DDX58 (RIG-I), which in turn activate expression and secretion of interferons including interferon α and interferon β (16). Interferons bind to their cognate receptors on neighboring cells and lead to activation of STAT1 and STAT2 through phosphorylation. Our western blot results showed elevated STAT1 level in arid4bΔ mESCs (day 0 of differentiation) (Figure 4a). Following exit from pluripotency, in both cell type, STAT1 levels declined although they still remained higher in arid4bΔ cells than in wild-type. Since interferon pathway activation correlated with the active phosphorylated STAT1 (pSTAT1), we compared its level in wild-type or arid4bΔ cells. At the mESC stage, there was a dramatic increase in pSTAT1 upon ARID4B loss. Mirroring total STAT1 level, the phosphorylated form was reduced upon endoderm differentiation. However, arid4bΔ cells had markedly more pSTAT1 than wild-type, even during differentiation.

Pluripotency of mESCs is regulated through a related STAT protein, STAT3 (17). We wanted to test whether the effect seen in arid4bΔ mESCs is specific to STAT1 or it also affects the STAT3 pathway. Unlike STAT1, total and phosphorylated forms of STAT3 were similar in wild-type and arid4bΔ cells at the mESC stage and through endoderm commitment (Figure 4b). These results show that the transcriptional upregulation of the pathway, originally observed through our RNA-seq results, is indicative of interferon-related STAT1 pathway activation in arid4bΔ cells.

We next wondered what the mechanism behind ARID4B-dependent regulation of interferon signaling was. To investigate this, changes in the chromatin environment of target genes were compared in endoderm committed cells (day 5). ChIP experiments were done for H3K4me3, H3K27Ac and H3K27me3 marks in wild-type or arid4bΔ endoderm cells (11). H3K4me3 and H3K27Ac generally correlates with active transcription while H3K27me3 plays a suppressive role (9). Our results suggest unique chromatin-based mechanisms lead to upregulation of target genes. For example, *OASL2* did not show a change in H3K4me3 or H3K27me3 level but had higher H3K27Ac in arid4bΔ cells, presumably leading to higher transcript levels (Figure 5a). The *STAT1* region had elevated H3K27Ac markers concomitant with decreased H3K27me3 (Figure 5b). In comparison, *DDX58* and *IRGM2* only had marked H3K4me3 increase in arid4bΔ cells (Figure 5c, d), while in *OAS1A* and *IFITM3*, H4K4me3 increase was accompanied with a similar increase in H3K27Ac (Figure 5e, f).

In order to understand which of these histone marks is more specifically associated with interferon pathway activation in arid4bΔ cells, we performed GREAT analysis (Stanford University) for ChIP-seq DNA sequences. This tool associates ChIP peaks with nearby genes and surveys a possible pathway enrichment. We performed GREAT for H3K4me3, H3K27me3 and H3K27Ac ChIP results in comparison with arid4bΔ over wild-type. We found that relevant pathways, such as defense response to virus, immune effector process and innate immune response, were only enriched in regions with higher H3K4me3 level in arid4bΔ cells over wild-type (Figure 5g). Although increase in H3K27Ac or loss of H3K27me3 markers were seen in individual target genes (Figure 5a, b, e, f), our results indicate a more generalized effect on H3K4me3 leads to interferon pathway activation upon ARID4B loss.

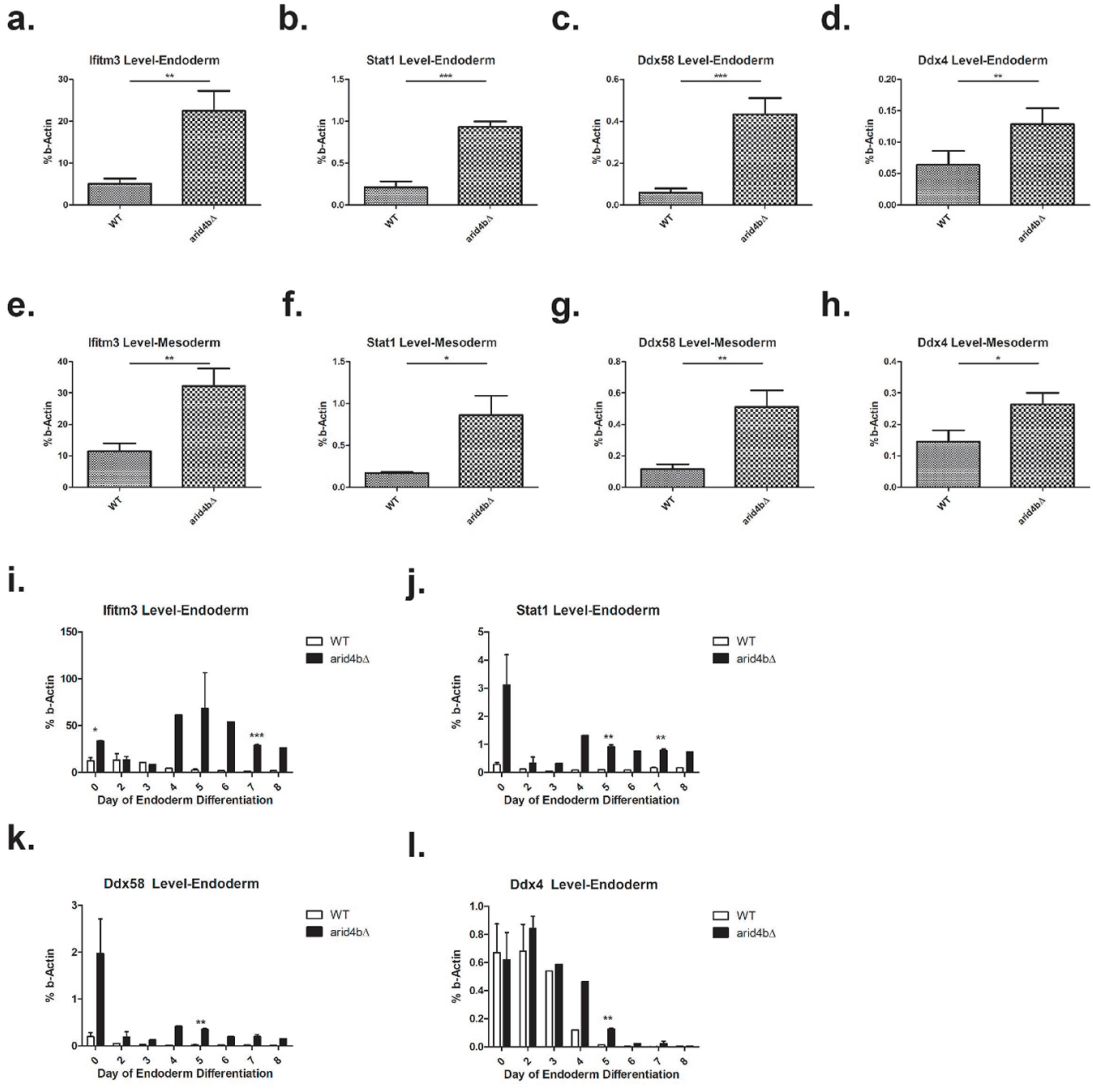

Figure 3. Validation of the expression of relevant differentially upregulated genes in arid4bΔ cells. RT-qPCR of *IFITM3*, *STAT1*, *DDX58* and *DDX4* in wild-type or arid4bΔ cells on day 5 of endoderm (a-d) or mesoderm (e-h) differentiation. RT-qPCR of *IFITM3* (i), *STAT1* (j), *DDX58* (k) and *DDX4* (l) during detailed endoderm differentiation time-course in wild-type or arid4bΔ cells. Statistical analyses (t-test) were done using GraphPad Prism software (*: p≤0.05, **: p≤0.01, ***: p≤0.001)
RT-qPCR: Real-time quantitative polymerase chain reaction

Discussion

Our previous results showed a clear mESC differentiation defect upon ARID4B loss. Derepression of lineage-specific meso/endoderm TF was not observed in arid4bΔ cells, despite cytokine-directed differentiation conditions.

We had previously investigated TF binding motifs enriched in our ChIP results (15). No particular TF motif was found enriched in H3K4me3 or H3K27me3 ChIP peaks. Interestingly, STAT1::STAT2 binding motif was enriched in regions with higher H3K27Ac level in arid4bΔ cells. When the ChIP peaks were separated based on their distance to transcription start site, it became clear that the H3K27Ac increases in arid4bΔ cells coincided with STAT1::STAT2 binding sites in promoter-distal regions that are presumably enhancers.

Viral RNA and DNA sensors in the cytoplasm initiate the antiviral response that leads to type I interferon (interferon α, β) expression (16). Secreted interferons bind to IFNAR 1-2 receptors through autocrine and paracrine mechanisms and activate JAK1-TYK2. This leads to phosphorylation of STAT1 and its nuclear translocation to transcribe interferon-stimulated genes.

mESCs naturally have limited antiviral response, at least partially due to the low levels of viral RNA sensors and inactive nuclear factor kappa B (18-20). Type 1 interferon pathway becomes mature coincident with mESC differentiation. Although intrinsic

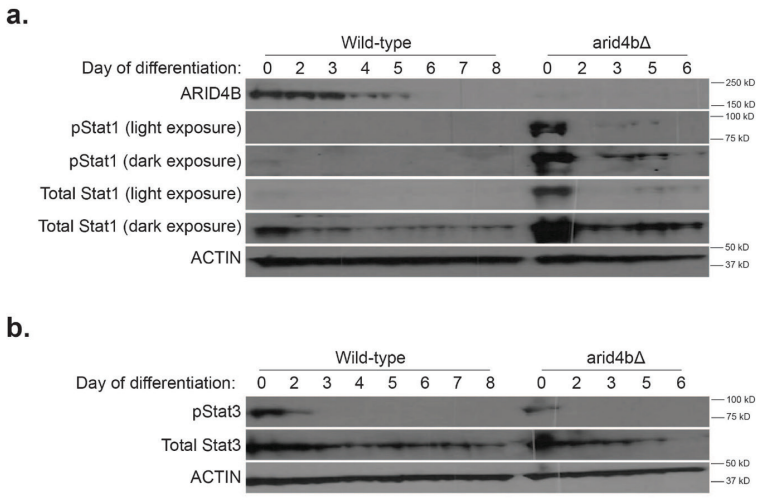

Figure 4. ARID4B loss leads to increased STAT1 level and activation at the mESC stage and during endoderm differentiation. (a) Western blot of ARID4B, STAT1, pSTAT1 (Tyr701) and loading control ACTIN using wild-type and arid4bΔ cell lysates during endoderm differentiation time-course, (b) Western blot of STAT3, pSTAT3 (Tyr705) and loading control ACTIN using wild-type and arid4bΔ cell lysates during endoderm differentiation time-course. Day 0 of differentiation represents the mESC stage

mESC: Mouse embryonic stem cell

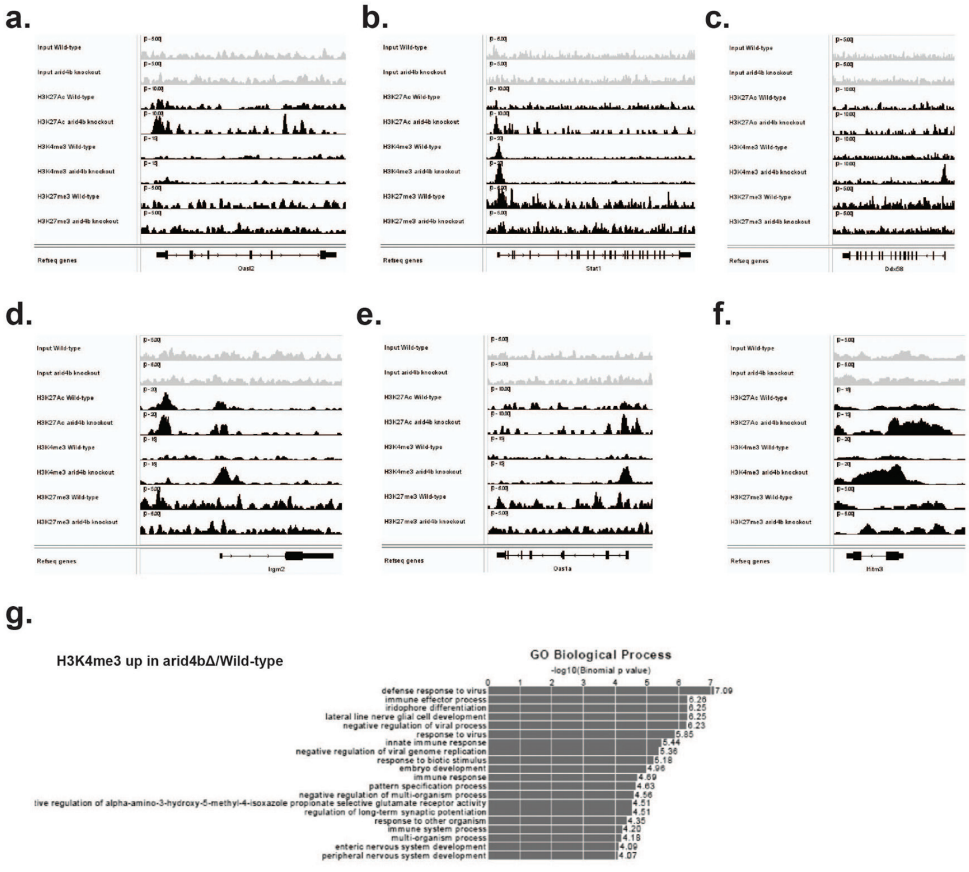

Figure 5. ARID4B loss results in changes in the chromatin landscape of relevant interferon-related genes. Integrative Genomics Viewer visualization of ChIP-seq tracks for selected interferon-related genes [*OASL2* (a), *STAT1* (b), *DDX58* (c), *IRGM2* (d), *OAS1A* (e), *IFITM3* (f)] in endoderm-directed WT and ARID4BΔ cells. *y* axes of WT and ARID4BΔ tracks are set to the same data range, (g) Genomic Regions Enrichment of Annotations Tool analysis of H3K4me3 ChIP-seq results upregulated in arid4bΔ cells over wild-type

low expression of interferon-stimulated genes independent of viral infection was recently reported in mESCs, this was shown to be dependent on the TF, IRF9 (21). We did not observe a change in *IRF9* transcript level in the absence of ARID4B, suggesting other mechanisms that include ARID4B in ISG regulation might be at play.

Our RNAseq results show no significant change in the level of sensor, interferon β or receptors. Instead, we observed a dramatic increase in STAT1 and interferon-stimulated gene transcript levels. This argues against an active viral response in arid4bΔ mESCs but suggests an aberrant transcriptional response due to high *STAT1* expression. Interestingly, in addition to *STAT1* mRNA levels, its protein, as well as active (phosphorylated) levels, are also elevated. Since JAK1 phosphorylates STAT1, this presumably points to the presence of other interferons that are secreted and can activate IFNAR-JAK receptor-kinase axis. Consistent with this, the less well studied interferon ϵ, interferon κ and interferon ω can also bind to IFNAR1/2 (22).

Our time-course RT-qPCR analysis of ARID4BΔ cells showed interferon-related genes have different expression kinetics through endoderm differentiation and in comparison to wild-type. Out of four genes tested, *STAT1* and *DDX58* had highest, though variable, arid4bΔ/wild-type expression difference in mESC stage. *IFITM3* and *DDX4*, on the other hand, reached highest arid4bΔ/wild-type expression difference later in endoderm differentiation. These differences might reflect the roles of the genes in early versus late interferon pathway activation. As one of the main TF of the interferon pathway, STAT1 is higher in the pathway hierarchy compared to the rest of the tested genes (16). Consistent with our data, it was reported that some interferon-related genes including *IFITM3* were expressed in mESCs without prior viral infection (19). Nevertheless, the expression of many interferon-related genes were altered during ESC differentiation (18,19). At the exit from pluripotency, IRF1 was shown to activate some interferon pathway genes including *DDX58* (21).

Alternatively, the differences might be due to the chromatin environment of these genes. The effect of ARID4B loss in the chromatin environment might be more or less permissive for efficient transcription. Consistently, we observed a decrease in H3K27me3 level that accompanied H3K4me3 increase in arid4bΔ cells in *STAT1* and *DDX58*. On the other hand, there was some residual, if not elevated, level of H3K27me3 in arid4bΔ cells in *IFITM3*, presumably dampening the transcriptional upregulation.

We found that H3K4me3 increase was associated strongly with interferon response and immune response pathway activations in arid4bΔ cells while H3K27me3 decrease or H3K27Ac increase did not lead to any related pathway enrichments. This result argues against a direct link between ARID4B and the altered chromatin environment of these pathway genes, since ARID4B is part of the RPD3L histone deacetylase complex. It is also possible that the heterogenous chromatin landscape of interferon-related genes masks direct effect of ARID4B. In fact, we found such differences in the IGV results. ARID4B-dependent histone acetylation changes might lead to a transcriptionally permissive environment that is conducive to H3K4me3 accumulation before or coincident with transcription activation. Since both histone acetylation and H3K4me3 is correlative with transcription (9), it is possible our results reflect a downstream rather than an immediate direct effect of ARID4B at these gene loci.

We observed higher antiviral response in endoderm committed arid4bΔ cells compared to mesoderm committed arid4bΔ cells. Although mesoderm and endoderm lineages originate from a common embryonic structure and thus share early progenitors, endoderm emergence occurs later during embryonic development. It is conceivable that the higher level of interferon-related gene expression in arid4bΔ cells in endoderm differentiation reflects the further maturation of an antiviral response through the differentiation timeline.

Previous reports identified the effect of histone deacetylation and STAT1 expression and transcription activity (23-25). Since ARID4B is part of the RPD3 histone deacetylase complex, our results are consistent with these findings and underline a possible link between STAT1 activity and mESC differentiation. Histone acetyltransferases and deacetylases can modify proteins other than histones (26). Another connection between acetylation and an interferon pathway comes from STAT1 post-translational modifications. Along with phosphorylation, STAT1 activity can be modulated by acetylation at its DNA-binding domain (27-29). Acetylation follows STAT1 phosphorylation and dampens its prolonged transcriptional activity. Our data is consistent with a model where the loss of ARID4B and its deacetylase complex might extend the duration of active STAT1 bound to its target genes, resulting in high level interferon-stimulated gene expression.

Study limitations

Our results show high expression of interferon related genes in arid4bΔ mESCs and differentiating cells. We found STAT1 protein level and its phosphorylated active form to be elevated in arid4bΔ cells. To gain a more comprehensive perspective on pathway activation, other proteins involved in STAT1 phosphorylation and downstream pathway activation would need to be verified through Western blot analysis.

Conclusion

Overall, we present evidence of transcript, protein and pathway level activation of interferon response, specifically through STAT1, in ARID4B-deficient mESCs through endoderm differentiation. Furthermore, our results show that the chromatin environment of interferon related genes is altered through changes, predominantly in H3K4me3 and H3K27Ac and to a lesser extent H3K27me3. Collectively, our data points to a role of ARID4B in the suppression of innate immune response via STAT1 through H3K4me3 and H3K27Ac regulation in mESCs and during endoderm differentiation.

Ethics Committee Approval: *Ethics committee approval form or institutional review board forms were not required.*

Informed Consent: *Informed consent approval form were not required.*

Peer-review: *Externally peer-reviewed.*

Financial Disclosure: *The author declared that this study received no financial support.*

References

1. Irion S, Nostro MC, Kattman SJ, Keller GM. Directed differentiation of pluripotent stem cells: from developmental biology to therapeutic applications. Cold Spring Harb Symp Quant Biol 2008; 73: 101-10.
2. Kalkan T, Smith A. Mapping the route from naive pluripotency to lineage specification. Philos Trans R Soc Lond B Biol Sci 2014; 369: 20130540.
3. Orkin SH, Wang J, Kim J, Chu J, Rao S, Theunissen TW, Shen X, et al. The transcriptional network controlling pluripotency in ES cells. Cold Spring Harb Symp Quant Biol 2008; 73: 195-202.
4. Keller GM. In vitro differentiation of embryonic stem cells. Curr Opin Cell Biol 1995; 7: 862-9.
5. Lewis SL, Tam PP. Definitive endoderm of the mouse embryo: formation, cell fates, and morphogenetic function. Dev Dyn 2006; 235: 2315-29.
6. Gadue P, Huber TL, Paddison PJ, Keller GM. Wnt and TGF-beta signaling are required for the induction of an in vitro model of primitive streak formation using embryonic stem cells. Proc Natl Acad Sci U S A 2006; 103: 16806-11.
7. Ying QL, Stavridis M, Griffiths D, Li M, Smith A. Conversion of embryonic stem cells into neuroectodermal precursors in adherent monoculture. Nat Biotechnol 2003; 21: 183-6.
8. Orkin SH, Hochedlinger K. Chromatin connections to pluripotency and cellular reprogramming. Cell 2011; 145: 835-50.
9. Li B, Carey M, Workman JL. The role of chromatin during transcription. Cell 2007; 128: 707-19.
10. Dixon JR, Jung I, Selvaraj S, Shen Y, Antosiewicz-Bourget JE, Lee AY, et al. Chromatin architecture reorganization during stem cell differentiation. Nature 2015; 518: 331-6.
11. Terzi Cizmecioglu N, Huang J, Keskin EG, Wang X, Esen I, Chen F, et al. ARID4B is critical for mouse embryonic stem cell differentiation towards mesoderm and endoderm, linking epigenetics to pluripotency exit. J Biol Chem 2020; 295: 17738-51.
12. Fleischer TC, Yun UJ, Ayer DE. Identification and characterization of three new components of the mSin3A corepressor complex. Mol Cell Biol 2003; 23: 3456-67.
13. Balbasi E, Guven G, Terzi Cizmecioglu N. Mouse Embryonic Stem Cell Culture in Serum-Containing or 2i Conditions. Methods Mol Biol 2022; 2520: 275-94.
14. Balbasi E, Sezginmert D, Alganatay C, Terzi Cizmecioglu N. Directed Differentiation of Mouse Embryonic Stem Cells to Mesoderm, Endoderm, and Neuroectoderm Lineages. Methods Mol Biol 2022; 2520: 295-307.
15. Keskin EG, Huang J, Terzi Çizmecioğlu N. Arid4b physically interacts with Tfap2c in mouse embryonic stem cells. Turk J Biol 2021; 45: 162-70.
16. Samuel CE. Antiviral actions of interferons. Clin Microbiol Rev 2001; 14: 778-809.
17. Zhang Y, Wang D, Xu J, Wang Y, Ma F, Li Z, et al. Stat3 activation is critical for pluripotency maintenance. J Cell Physiol 2019; 234: 1044-51.
18. D'Angelo W, Gurung C, Acharya D, Chen B, Ortolano N, Gama V, et al. The Molecular Basis for the Lack of Inflammatory Responses in Mouse Embryonic Stem Cells and Their Differentiated Cells. J Immunol 2017; 198: 2147-55.
19. Wu X, Dao Thi VL, Huang Y, Billerbeck E, Saha D, Hoffmann HH, et al. Intrinsic Immunity Shapes Viral Resistance of Stem Cells. Cell 2018; 172: 423-38.
20. Wang R, Wang J, Paul AM, Acharya D, Bai F, Huang F, et al. Mouse embryonic stem cells are deficient in type I interferon expression in response to viral infections and double-stranded RNA. J Biol Chem 2013; 288: 15926-36.
21. Romeike M, Spach S, Huber M, Feng S, Vainorius G, Elling U, et al. Transient upregulation of IRF1 during exit from naive pluripotency confers viral protection. EMBO Rep 2022; 23: e55375.
22. Harris BD, Schreiter J, Chevrier M, Jordan JL, Walter MR. Human interferon-ϵ and interferon-κ exhibit low potency and low affinity for cell-surface IFNAR and the poxvirus antagonist B18R. J Biol Chem 2018; 293: 16057-68.
23. Gonneaud A, Turgeon N, Jones C, Couture C, Lévesque D, Boisvert FM, et al. HDAC1 and HDAC2 independently regulate common and specific intrinsic responses in murine enteroids. Sci Rep 2019; 9: 5363.
24. Filgueiras LR, Brandt SL, Ramalho TR, Jancar S, Serezani CH. Imbalance between HDAC and HAT activities drives aberrant STAT1/MyD88 expression in macrophages from type 1 diabetic mice. J Diabetes Complications 2017; 31: 334-9.
25. Klampfer L, Huang J, Swaby LA, Augenlicht L. Requirement of histone deacetylase activity for signaling by STAT1. J Biol Chem 2004; 279: 30358-68.
26. Glozak MA, Sengupta N, Zhang X, Seto E. Acetylation and deacetylation of non-histone proteins. Gene 2005; 363: 15-23.
27. Tang X, Gao JS, Guan YJ, McLane KE, Yuan ZL, Ramratnam B, et al. Acetylation-dependent signal transduction for type I interferon receptor. Cell 2007; 131: 93-105.
28. Krämer OH, Baus D, Knauer SK, Stein S, Jäger E, Stauber RH, et al. Acetylation of STAT1 modulates NF-kappaB activity. Genes Dev 2006; 20: 473-85.
29. Kumar P, Gogulamudi VR, Periasamy R, Raghavaraju G, Subramanian U, Pandey KN. Inhibition of HDAC enhances STAT acetylation, blocks NF-κB, and suppresses the renal inflammation and fibrosis in Npr1 haplotype male mice. Am J Physiol Renal Physiol 2017; 313: F781-95.